The Conference on Pedestrian and Evacuation Dynamics 2014 (PED2014)

The visual coupling between neighbors in real and virtual crowds

Kevin Rio [a,*], William H. Warren [a]

[a] *Dept. of Cognitive, Linguistic, & Psychological Sciences, Brown University, 190 Thayer St., Providence RI 02906, USA*

Abstract

Many models of crowd behavior are based on local interactions between pedestrians, but little is known about the actual mechanisms governing these interactions. In Experiments 1 and 2, a participant walked with three human 'confederates' or a virtual crowd of 30, while the heading direction or speed of a subset of neighbors was manipulated. In Experiment 3, real crowds of 16 or 20 walked together in a swarming scenario. We find that pedestrians are unidirectionally coupled to neighbors ahead of them, the influence of multiple neighbors is linearly combined, and their weights decrease with distance.

1. Introduction

Human crowds are self-organized complex systems in which global patterns of collective behavior are believed to emerge from local interactions between pedestrians and their environment (Sumpter et al. (2012)). The study of crowd behavior, and collective motion more generally, has become a highly interdisciplinary endeavor, with efforts from animators (Reynolds (1987)), biologists (Huth and Wissel (1994); Couzin and Krause (2003); Couzin (2009); Lukeman et al. (2010)), computer scientists (Paris et al. (2007); Ondřej et al. (2010)), theoretical physicists (Helbing and Molnar (1995); Czirók and Vicsek (2000)), transport engineers (Daamen and Hoogendoorn (2003)), and many others. The understanding of collective behavior has been advanced tremendously by theoretical models and large-

* Corresponding author. Tel.: +1-401-863-2727; fax: +1-401-863-2255.
  E-mail address: kevin_rio@brown.edu

scale simulations, but there is a growing consensus that this effort must be informed by rigorous observational and experimental studies to specify the local rules or control laws that give rise to global phenomena.

Driven in part by recent advances in tracking technologies, there is a rising tide of data-driven approaches to collective behavior, including work on fish schools (Ward et al. (2008)), bird flocks (Ballerini et al. (2008); Cavagna et al. (2010)), as well as pedestrian behavior (Moussaid et al. (2009); Lemercier et al. (2012); Rio et al. (2014)) and crowd dynamics (Moussaid et al. (2010); Bonneaud et al. (2012)) in humans. Data can be utilized in many ways, from calibrating the parameters of proposed models (Johansson et al. (2007)) to identifying the information individual agents utilize to guide behavior (Ballerini, et al. (2008)).

Previously, we have advocated for an experimental approach to collective behavior that begins by developing dynamical models of simple pedestrian interactions (Fajen and Warren (2003); Fajen and Warren (2007); Rio et al. (2014)), extends them to more complex scenarios (Kiefer et al. (2013)), and ultimately uses them to predict patterns of crowd dynamics (Bonneaud et al. (2014)). We recently showed that a pedestrian follows a neighbor by matching the leader's speed and heading direction, based on visual information (Rio et al. (2014); Dachner and Warren (2014)). Here, we present three studies that seek to map out the visual coupling between a pedestrian and multiple neighbors in a crowd, and determine how their influence is combined. In Experiment 1, we manipulated the walking speed and direction of three human 'confederates' and observed their influence on the behavior of a participant as they walked together in a group. In Experiment 2, we built upon these results by manipulating a virtual crowd as a participant walked in ambulatory virtual reality. Finally, in Experiment 3, we collected naturalistic data on real crowds walking in a 'swarm' scenario. Our aim is to derive cognitively-plausible, empirically-grounded models of local pedestrian behavior and use them to generate realistic patterns of global crowd behavior, predicated on the perceptual-motor capabilities of human agents.

2. Experiment 1: Walking in a Small Crowd of Confederates

The purpose of the first experiment was to investigate the coupling between a pedestrian and a few neighbors (N=3) by manipulating the heading direction (turn left, turn right) or speed (speed up, slow down) of a subset of confederates. We varied the number of confederates in the subset (0, 1, 2, 3), the eccentricity of the single confederate (center, side), and the initial distance between pedestrians (1, 2 m).

2.1. Methods

Participants. Ten participants, 4 female and 6 male, were recruited for Experiment 1. None reported having any visual or motor impairment, and they were paid for their participation. A separate group of three trained experimenters, 2 female and 1 male, acted as confederates in the experiment.

Apparatus. The research was conducted in the Virtual Environment Navigation Laboratory (VENLab) at Brown University. The participant and confederates walked diagonally across in a 12x14 m room, and each wore a set of wireless headphones connected to a PC that delivered pre-recorded instructions. Head position and orientation were recorded at a sampling rate of 60 Hz using a hybrid ultrasonic-inertial tracking system (IS-900, Intersense, Billerica MA) affixed to the headphones. (Note that virtual displays were not used in this experiment.) Eight starting positions were marked on the floor with pieces of colored tape, arranged in two concentric diamond configurations with initial distances of 1 and 2 m on a side (see Fig. 1).

Procedure. Participants in Experiment 1 were not informed of confederates' complicity in the experiment. All four pedestrians (the participant and three confederates) received the same verbal instructions at the beginning of the experiment; they were told simply to "walk together across the room."

On each trial, the four pedestrians were directed via wireless headphones to go to one of the 8 starting locations. Only trials in which the participant was located in the back position (i.e. the rear vertex of the diamond) were analyzed further. In addition, the confederates were covertly instructed to "turn left," "turn right," "speed up," or "slow down," on each trial. The same instruction was given to a subset of the confederates (1, 2, or 3), depending on the condition; to avoid collisions, in the subset = 1 condition the Right confederate was instructed to "turn right," and in the subset = 2 condition the Right and Center confederates were instructed to "turn right" (and vice versa).
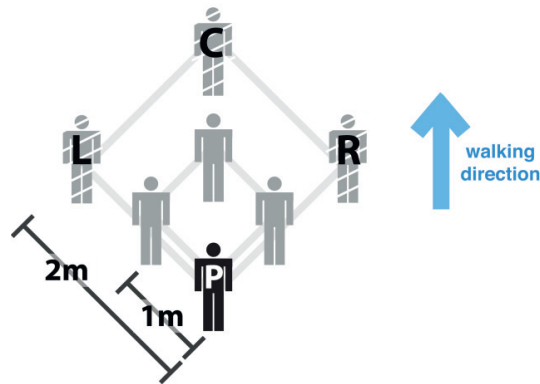
Fig. 1. Initial conditions of participant (P) and three confederates (L, C, R) in Experiment 1.

The trial began when a verbal command ("Begin") instructed all four pedestrians to start walking across the room. When the first confederate crossed an invisible line located 4 m in front of the participant's starting location, the subset of confederates heard a pure tone indicating they should initiate the speed or heading change. They maintained this speed or direction for the duration of the trial. Once the first confederate reached the opposite side of the room (about 13m), all four pedestrians received a verbal command ("End"), indicating the end of the current trial, and instructions for the next trial were presented.

Design. Experiment 1 had a 2 (initial distance) x 2 (heading or speed change) x 9 (confederate manipulations) design. Because some heading change conditions were removed to avoid collisions (see Procedure), there were 32 heading change trials (8 conditions x 4 repetitions per condition), 24 speed change trials (12 conditions x 2 repetitions per condition) and 8 no-change control trials, for a total of 64 trials per participant.

Data analysis. The time series of head position for all four pedestrians were recorded in three dimensions, but only data in the horizontal *xy*-plane were analyzed. Each time series was low-pass filtered using a forward and backward 4th-order low-pass Butterworth filter with a cutoff frequency of 1Hz, to reduce occasional tracker error and attenuate anterior-posterior accelerations due to the step cycle. To eliminate edge effects from filtering at the end of the trial ('endpoint error'), the position time series were extended by 2 s using linear extrapolation based on the last 0.5 s of data (Vint and Hinrichs (1996); Howarth and Callaghan (2009)); the extrapolated portions were not included any subsequent analysis. The filtered position data were used to compute time series of speed, heading, and acceleration.

2.2. Results

Descriptive. Participants responded to manipulations of the confederates' behavior. Measuring the participant's final lateral position or final speed relative to control trials (Fig. 2) reveals that overall, the participant turned left (or right) when one or more confederates did so, and sped up (or slowed down) when one or more confederates did. Two-way ANOVAs on final position and final speed, with the confederate manipulation and initial distance as factors, confirmed a significant main effect of the manipulation on both variables (position: $F_{(8,161)} = 28.82$, $p < .001$; speed: $F_{(8,160)} = 37.14$, $p < .001$). There was no effect of initial distance on final position ($F_{(1,161)} = 0.19$, $p > .05$), a marginal effect of initial distance on final speed ($F_{(1,160)} = 0.024$, $p = .06$), and no interactions (position: $F_{(8,161)} = 0.16$, $p > .05$; speed: $F_{(18160)} = 1.33$, $p > .05$).

Participant Final Position
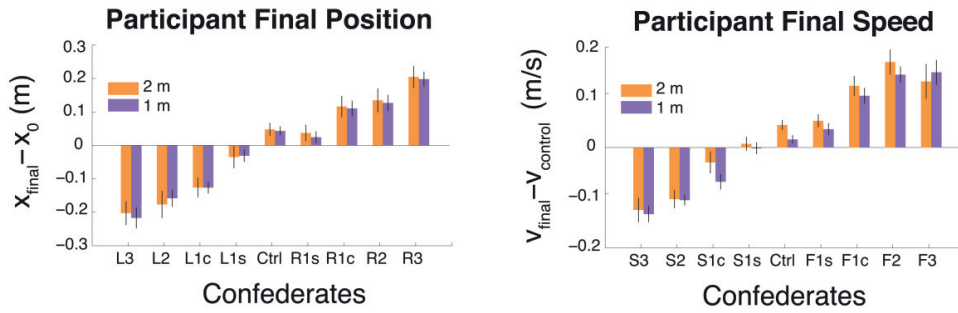
Participant Final Speed

Fig. 2. Mean changes in participants' final position (left panel) and speed (right panel) in Experiment 1.

Participants were not only sensitive to the direction of change in confederate motion, but also to the number of confederates in the subset and perhaps their eccentricity on each trial. Overall, participant response increased with the number of confederates that were manipulated, and was greater for confederates in the center position than for confederates in the left or right position. As an example, in response to the "turn right" confederate manipulation, participants' mean change in final position was small for 1 confederate (M = 0.07 m, SD = 0.12 m), greater for 2 confederates (M = 0.13 m, SD = 0.14 m), and greatest for 3 confederates (M = 0.21 m, SD = 0.18 m). Bonferroni post-hoc corrections revealed that the differences between 3 confederates and control, and between 3 confederates and 1 confederate, were significant ($p < .05$), while the difference between 3 confederates and 2 confederates was not significant ($p > .05$). The mean change in final position was greater with a single confederate in the center position (M = 0.11 m, SD = 0.13 m) than for a single confederate in the left or right position (M = 0.02 m, SD = 0.09 m), although this difference was not significant ($p > .05$). A similar pattern of results holds for the turn left, speed up, and slow down manipulations.

To estimate how the visual coupling depends on the number and eccentricity of neighbors, we performed a multiple linear regression of participant final positions on the 3 confederates' final positions, and a similar regression for final speed. This analysis showed that nearly half of the variance in participant final position ($R^2 = 0.43$, $p < .001$) and speed ($R^2 = 0.46$, $p < .001$) was accounted for by the confederate manipulations. The weight of the center confederate was greater than that of the left and right confederates for both heading ($w_L = 0.27$, $w_C = 0.47$, $w_R = 0.26$) and speed ($w_L = 0.19$, $w_C = 0.47$, $w_R = 0.34$).

Modeling and simulation. To better understand speed coordination in this experiment, we simulated the participants' walking trajectories using a dynamical model of speed control developed to account for following behavior in dyads (Rio et al. (2014)). In this model, the acceleration of the follower is a function of the difference in speed between the leader and the follower, with a gain *k*:

$$\ddot{x}_{follower} = k(\dot{x}_{leader} - \dot{x}_{follower}) \tag{1}$$

Generalizing this model to multiple neighbors, a simple pooling model would predict that the acceleration of the participant is a weighted linear combination of the difference in speed with each of the 3 confederates:

$$\ddot{x}_{participant} = k[w_L(\dot{x}_L - \dot{x}_p) + w_C(\dot{x}_C - \dot{x}_p) + w_R(\dot{x}_R - \dot{x}_p)] \tag{2}$$

Adopting the gain k from our previous dyad data and the weights *w* for eccentricity from the multiple regression on the present speed data, we simulated the participant's time series of acceleration on each trial using the 3 confederates' time series of speed as input. Not surprisingly, the trial-by-trial model fits based on the group input are lower (mean r = 0.28) than the previous fits with a single leader (mean r = 0.67). But the model closely reproduces the pattern of mean final speeds in Fig. 2, and differs only marginally ($F(1,213) = 3.44$, $p = .06$) from the human data, as shown in Fig. 3.
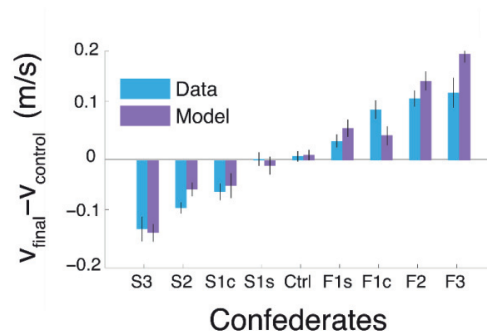

Fig. 3. Mean changes in participants' final speed; human data (blue) and model prediction (purple).

Overall, the results from Experiment 1 suggest that pedestrians are locally coupled to multiple neighbors and that their influence is linearly combined, weighted by eccentricity, with neighbors to the side having a weaker influence than neighbors in the direction of travel.

3. Experiment 2: Walking in a Virtual Crowd

The purpose of Experiment 2 was to scale up from a small group to a larger crowd (N=30) by taking advantage of virtual reality techniques, and similarly manipulate the heading (turn left, turn right) or speed (speed up, slow down) of a subset of virtual pedestrians. In this experiment, we varied the number of neighbors in the subset (0, 3, 6, 9, 12) and the density of the crowd (mean initial distance = 2.5 m or 5.5 m).

3.1. Methods

Participants. Ten participants, 6 female and 4 male, were recruited for Experiment 2, with the same criteria as before.

Apparatus. The participant walked in the VENLab while viewing a virtual environment through a wireless stereoscopic head-mounted display (Rift DK1, Oculus, Irvine CA) that provided a 110° diagonal field of view with a resolution of 640 x 800 pixels in each eye. Displays were generated on a Dell XPS workstation (Round Rock TX) at a frame rate of 60 fps, using the Vizard software package (WorldViz, Santa Monica CA). Head position and orientation were recorded at 60 Hz as before, and used to update the display with a latency of approximately 50 ms (three frames).

Displays. The virtual environment included a visual surround consisting of a ground plane mapped with a grayscale granite texture and a blue sky. A green home pole (radius 0.2 m, height 3 m) and a red orienting pole (radius 0.2 m, height 3 m) appeared at either extreme of the room's diagonal, 12.73 m apart. A crowd of 30 virtual pedestrians was generated using high-polygon (M = 8073, SD = 780), textured (2048 x 2048 pixels) 3D models; 12 of them were rendered within a participant's typical horizontal field of view (90°), while the other 18 were placed outside the field of view to enhance the sense of immersion. The latter could be seen if the participant turned their head (which was infrequent), but they were not manipulated and will be ignored in subsequent analyses. The virtual pedestrian models were animated with a walking gait, with an update rate of 60 frames per second. The virtual crowd contained equal numbers of men and women and diverse races and ethnicities.

Procedure. Participants in Experiment 2 were instructed to walk as naturally as possible, to treat the virtual pedestrians as if they were real, and to stay together with the crowd. To begin each trial, participants stood at the green home pole and faced the red orientating pole. After 2 s, the 12 virtual pedestrians appeared in front of the participant. 1 s later, a verbal command ("Begin") was heard over a loudspeaker, and the virtual pedestrians began walking. When the participant had walked about 12 m, a second verbal command ("End") signaled the end of the current trial.

Design. Experiment 2 had a 2 density (2.5 m or 5.5 m initial distance) x 2 change (heading or speed) x 2 direction of change (left/right or fast/slow) x 5 subset (0, 3, 6, 9, 12 neighbors) factorial design, for a total of 40 conditions. There were 4 repetitions per condition, for a total of 160 trials per participant.

Data analysis. Data were processed and analyzed as in Experiment 1.

3.2. Results

Participants again responded to the manipulation of neighbor heading and speed. Fig. 4 presents participants' mean changes in final position or final speed, relative to control trials. Overall, participants turned left (or right) when one subsets of virtual neighbors did so, and sped up (or slowed down) when neighbors did. A two-way ANOVA on final position, with the neighbor manipulation (number and direction) and initial density as factors, confirmed that there were significant main effects of heading change ($F(9,180) = 84.87$, $p < .001$) and density ($F(1,180) = 4.23$, $p < .05$), but no interaction ($F(9,180) = 1.11$, $p > .05$). The turning response again increased with the number of neighbors in the subset. For example, looking at the turn right manipulation, participants' mean change in position was lowest when 3 virtual pedestrians turned right ($M = 0.27$ m, $SD = 0.21$ m), and progressively increased when 6 ($M = 0.43$ m, $SD = 0.19$ m), 9 ($M = 0.72$ m, $SD = 0.20$ m), and 12 ($M = 0.85$ m, $SD = 0.22$ m) virtual pedestrians were manipulated. A similar pattern of results held for the turn left manipulation. There was also a slight rightward bias, and the main effect of density indicated that it was significantly greater in the low density ($M = 0.12$ m, $SD = 0.52$ m) than the high density ($M = 0.04$ m, $SD = 0.57$ m) condition.

A two-way ANOVA on final speed revealed a significant main effect of neighbor manipulation ($F(9,180) = 75.62$, $p < .001$), no main effect of density ($F(1,180) = 0.23$, $p > .05$), and a significant interaction ($F(9,180) = 2.79$, $p < .01$). This confirms a strong effect of number of neighbors in the subset. The interaction was driven primarily by greater acceleration in the high density condition; for example, the participant's change in speed was nearly twice as large when 12 neighbors sped up in the high density condition ($M = 0.27$ m/s, $SD = 0.09$ m/s) as in the low density condition ($M = 0.14$ m/s, $SD = 0.10$ m/s). In contrast, when 12 virtual neighbors slowed down, participant response was comparable in the high density ($M = -0.34$ m/s, $SD = 0.05$ m/s) and low density ($M = -0.27$ m/s, $SD = 0.11$ m/s) conditions.
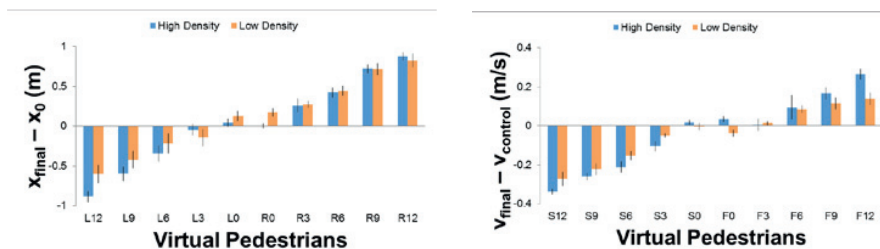

Fig. 4. Mean changes in participants' final position (left panel) and final speed (right panel) in Experiment 2.

Overall, the results of Experiment 2 indicate that pedestrians are locally coupled to as many as 12 neighbors, and that the influence of multiple neighbors seems to increase linearly with the number that change their walking direction or speed. Moreover, the influence of neighbors appears to persist even as the overall density of the crowd decreases, at least over the range of interpersonal distances tested.

4. Experiment 3: Interpersonal coordination in human 'swarms'

In Experiment 3, we sought to measure the coordination between neighbors in real human crowds. For this purpose, we collected motion capture data on up to 20 participants walking in a 'swarm' scenario, and analyzed pairwise statistics between a central participant and each neighbor.

4.1. Methods

Participants. A total of 36 participants was recruited over two sessions (N=16 and N=20 in each session, respectively) for Experiment 3, with the same criteria as before.

Apparatus. The experiment was conducted in a large hall at Brown University. Participants walked together in a 14 x 20 m tracking area, marked on the floor with red tape. Each wore a lightweight bicycle helmet with 5 reflective markers on protruding stalks in a unique constellation. A 16-camera infrared motion capture system (Qualisys Oqus, Deerfield IL) was used to record head position at a sampling rate of 60 Hz.

Procedure. Each group of participants was instructed to "walk about the room on a random path at a normal speed, while staying together as a group, veering left or right, for a couple of minutes." They were also told to stay within the tracking area. There were no designated leaders, and there was no external signal about when to turn. Participants began each trial by randomly arranging themselves within one of two start boxes (4x4 m or 7x7 m), which defined two initial densities (high and low, respectively).

Design. Each group of participants completed 4 trials (2 low density, 2 high density), each lasting 120 s (2 min). This yielded a total of 1,152,000 data points.

Data analysis. 3D head positions on each frame were recovered from the motion capture data using a specifically designed algorithm. The unique 'constellation' of markers was used to identify each helmet. Across all trials and participants, head position was recovered on 88% of frames, and the data were then processed as before.

4.2. Results

Global coordination. As global measures of heading coordination, we computed group polarization and group angular momentum (Couzin, et al., 2002), which purportedly capture linear alignment and circular alignment, respectively. Both measures range from 0 to 1, with 0 representing either no coordination or coordination in opposing directions, and 1 representing perfect coordination; see Fig. 5.

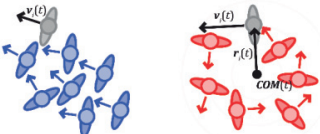$$P(t) = \frac{1}{N} \left| \sum_{i=1}^{N} \boldsymbol{v}_i(t) \right| \qquad M(t) = \frac{1}{N} \left| \sum_{i=1}^{N} \boldsymbol{r}_i(t) \times \boldsymbol{v}_i(t) \right|$$

Fig. 5. Group polarization (left panel) and group angular momentum (right panel), two global measures of coordination.

As illustrated in Fig. 6, polarization was generally higher (M = 0.86, SD = 0.13) than angular momentum (M = 0.17, SD = 0.20). There was no reliable trade-off between the two measures; although angular momentum sometimes increased when polarization decreased (and vice versa), this was not always the case. This may reflect the observation that there were gradual transitions between linear and curved alignments from the front to rear of the swarm, such that both were often present simultaneously. We note that the angular momentum measure is based on a circular configuration of pedestrians, which is not typical of the swarm.
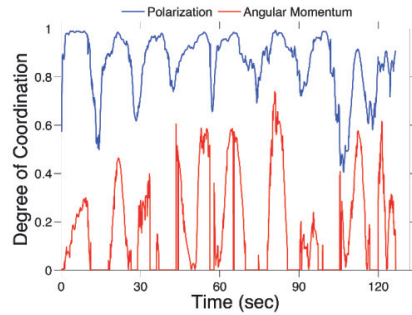
Fig. 6. Group polarization (blue) and group angular momentum (red) for a representative trial in Experiment 3.

Local coordination. To investigate the local coordination between pedestrians in the swarm, we computed pairwise statistics on each frame and aggregated them across frames and trials. Many of these statistics were computed between the 'focal' pedestrian (the pedestrian nearest to the center of the swarm on each frame) and each neighbor. This approach minimizes edge effects that can occur with focal pedestrians on the edge of the swarm (Cavagna et al., 2010).

An occupancy grid for 6 min of swarm data appears in Fig. 7 (left), plotted in the focal pedestrian's coordinate frame. The origin (0,0) is the focal pedestrian's location, the positive y-axis (up) is aligned with their heading direction, and color corresponds to the percentage of frames that neighbors are found in each cell. There appears to be an exclusion zone with radius 0.5 m, in which neighbors almost never appear, surrounded by a 'preferred' zone with radius 1-2 m where neighbors are most often found. It is possible that these zones indicate a preferred interpersonal distance in human crowds, consistent with distance-based attraction/repulsion models (Schellinck and White (2011)). However, they may simply reflect the initial density of the swarm in the present experiment. Further manipulation of initial density will test the invariance of these zones.

The heat map in Fig. 7 (right) represents the mean absolute difference in heading between the focal pedestrian and all neighbors for 6 min of data, plotted in the focal pedestrian's coordinate frame. This vividly depicts the degree of heading alignment, providing an estimate of the coupling strength in the focal participant's neighborhood. Notably, the heading difference is small (<20°) within a radius of about 2 m, and nearly doubles (35-40°) by 4 m, indicating a strong local coupling that decays rapidly with distance. Whether this decay is due to metric distance or to occlusion by intervening neighbors remains to be determined by manipulating swarm density. The circularly symmetric pattern offers little suggestion of an eccentricity effect.

Overall, the analysis of the swarm data show that human crowds exhibit coherent global patterns of coordination, and the pairwise statistics further reveal properties of the local interactions between neighbors, such as a strong local coupling that is circularly symmetric and decreases with increasing radial distance.
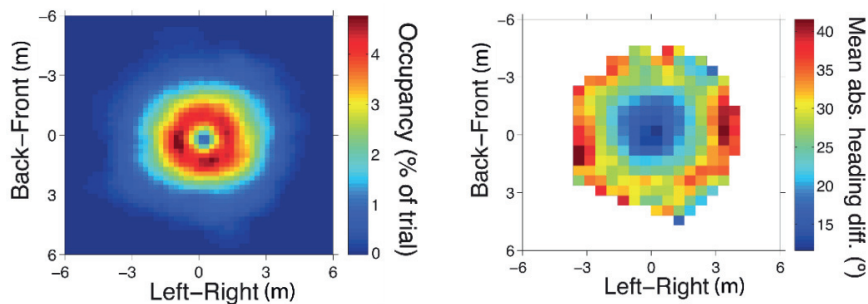

Fig. 7. Occupancy grid (left panel) and heat map of mean absolute heading difference (right panel) in Experiment 3.

5. Conclusion

We have presented data from three experiments that systematically investigated the local visual coupling between neighbors in a crowd. Experiment 1 and 2 found that pedestrians are locally coupled to their neighbors, and that the influence from multiple neighbors is linearly combined; Experiment 1 suggested that coupling strength depends on eccentricity, and Experiment 2 showed that this coupling extends to as many as 12 neighbors. Experiment 3 found that this local coupling also exists in larger crowds, and can be quantified using global measures and pairwise statistics. Taken together, these results provide an empirical basis for selecting, calibrating, and validating models of the local interactions between pedestrians, which form the foundation for many models of global crowd behavior.

References

Ballerini, M., Cabibbo, N., Candelier, R., Cavagna, A., Cisbani, E., Giardina, I., ... Zdravkovic, V., 2008. Interaction ruling animal collective behavior depends on topological rather than metric distance: Evidence from a field study.Proceedings of the National Academy of Sciences 105(4), 1232-1237.

Bonneaud, S., Rio, K., Chevaillier, P., Warren, W.H., 2012. Accounting for patterns of collective behavior in crowd locomotor dynamics for realistic simulations. In Transactions on Edutainment VII (pp. 1-11). Springer Berlin Heidelberg.

Cavagna, A., Cimarelli, A., Giardina, I., Parisi, G., Santagati, R., Stefanini, F., Viale, M., 2010. Scale-free correlations in starling flocks. Proceedings of the National Academy of Sciences 107(26), 11865-11870.

Couzin, I.D., 2009. Collective cognition in animal groups. Trends in Cognitive Sciences 13(1), 36-43.

Couzin, I.D., Krause, J., 2003. Self-organization and collective behavior in vertebrates. Advances in the Study of Behavior, 32(1).

Czirók, A., Vicsek, T., 2000. Collective behavior of interacting self-propelled particles. Physica A: Statistical Mechanics and its Applications 281(1), 17-29.

Daamen, W., Hoogendoorn, S.P., 2003. Experimental research of pedestrian walking behavior. Transportation Research Record: Journal of the Transportation Research Board 1828(1), 20-30.

Dachner, G., Warren, W.H., 2014. Behavioral dynamics of heading alignment in pedestrian following. Transportation Research Procedia, 00, 00-00.

Fajen, B.R., Warren, W.H., 2003. Behavioral dynamics of steering, obstacle avoidance, and route selection. Journal of Experimental Psychology: Human Perception and Performance 29(2), 343.

Fajen, B.R., Warren, W.H., 2007. Behavioral dynamics of intercepting a moving target. Experimental Brain Research 180(2), 303-319.

Helbing, D., Molnar, P., 1995. Social force model for pedestrian dynamics. Physical Review E 51(5), 4282.

Howarth, S.J., Callaghan, J.P., 2009. The rule of 1s for padding kinematic data prior to digital filtering: Influence of sampling and filter cutoff frequencies. Journal of Electromyography and Kinesiology 19(5), 875-881.

Huth, A., Wissel, C., 1994. The simulation of fish schools in comparison with experimental data. Ecological modelling, 75, 135-146.

Lukeman, R., Li, Y. X., Edelstein-Keshet, L., 2010. Inferring individual rules from collective behavior. Proceedings of the National Academy of Sciences 107(28), 12576-12580.

Johansson, A., Helbing, D., Shukla, P. K., 2007. Specification of the social force pedestrian model by evolutionary adjustment to video tracking data. Advances in Complex Systems, 10, 271-288.

Kiefer, A. W., Bonneaud, S., Rio, K., Warren, W. H., 2014. Quantifying the Coherence of Pedestrian Groups. Proceedings of the Cognitive Science Society 35th Annual Meeting.

Lemercier, S., Jelic, A., Kulpa, R., Hua, J., Fehrenbach, J., Degond, P., ... Pettré, J., 2012. Realistic following behaviors for crowd simulation. In Computer Graphics Forum 31 (2), pp. 489-498.

Moussaïd, M., Helbing, D., Garnier, S., Johansson, A., Combe, M., Theraulaz, G., 2009. Experimental study of the behavioural mechanisms underlying self-organization in human crowds. Proceedings of the Royal Society B: Biological Sciences, rspb-2009.

Moussaïd, M., Perozo, N., Garnier, S., Helbing, D., Theraulaz, G., 2010. The walking behaviour of pedestrian social groups and its impact on crowd dynamics. PloS One 5(4), e10047.

Ondřej, J., Pettré, J., Olivier, A.H., Donikian, S., 2010. A synthetic-vision based steering approach for crowd simulation. In ACM Transactions on Graphics (TOG) 29(4), pp. 123.

Paris, S., Pettré, J., Donikian, S., 2007. Pedestrian reactive navigation for crowd simulation: a predictive approach. In Computer Graphics Forum, 26(3), pp. 665-674.

Rio, K.W., Rhea, C.K., Warren, W.H., 2014. Follow the leader: Visual control of speed in pedestrian following. Journal of Vision 14(2), 4.

Reynolds, C.W., 1987. Flocks, herds and schools: A distributed behavioral model. ACM SIGGRAPH Computer Graphics 21(4), 25-34.

Sumpter, D.J., Mann, R.P., Perna, A., 2012. The modelling cycle for collective animal behaviour. Interface Focus, rsfs.2012.0031.

Vint, P.F., Hinrichs, R.N., 1996. Endpoint error in smoothing and differentiating raw kinematic data: an evaluation of four popular methods. Journal of Biomechanics 29(12), 1637-1642.

Ward, A.J., Sumpter, D.J., Couzin, I.D., Hart, P.J., Krause, J., 2008. Quorum decision-making facilitates information transfer in fish shoals. Proceedings of the National Academy of Sciences 105(19), 6948-6953.